

RESEARCH PAPER

## Design of Bio-Prepared Nanoelectrochemical Sensors Using Plant Extracts for Detection of Heavy Metals in Industrial Water

Fatma H. Abdulla <sup>1\*</sup>, Zainab Talib Abd Al-Kadhum <sup>2</sup>, Dhuha T. Al-Sultani <sup>3</sup>

<sup>1</sup> Department of Biology, College of Science, University of Baghdad, Baghdad, Iraq

<sup>2</sup> Department of Plant Production Technologies, College of Al-Musaib Technical, University of Al-Furat Al-Awsat Technical, Babylon, Iraq

<sup>3</sup> Polymer Engineering and Petrochemical Industries Department, University of Babylon, Iraq

### ARTICLE INFO

#### Article History:

Received 09 March 2026

Accepted 19 May 2026

Published 01 July 2026

#### Keywords:

Electrochemical sensors

Green synthesis

Heavy metals

Nanoparticles

Plant extracts

Voltammetry

### ABSTRACT

This work was conducted to develop and test biosynthesized electrochemical nanosensors from the plants *Ficus elastica* and *Acalypha indica* for the detection of lead ( $Pb^{2+}$ ), cadmium ( $Cd^{2+}$ ), and mercury ( $Hg^{2+}$ ) ions in industrial wastewater, river water, and groundwater. Metal oxides and metal nanoparticles (CuO, Ag, and ZnO) were obtained from these sensors. Carbon paste (CPE) electrodes were modified using biosynthesized nanomaterials and polyaniline (PANI) to form the electrochemical sensors. The sensor voltage was measured using cyclic voltage (CV) and square wave voltage (SWV). The developed sensors exhibited detection limits ranging from 0.07 to 0.16  $\mu g/L$ . Sensor recovery rates on real, supported industrial water samples ranged from 97% to 104%, confirming the sensors' effectiveness and high analytical sensitivity. Green synthesis offers a cost-effective, environmentally friendly, and sustainable pathway for producing high-performance electrochemical sensors used in the field monitoring of heavy metals in industrial environments.

### How to cite this article

Dehghankelishadi B, Dorkoosh FA. Pluronic based nano-delivery systems; Prospective warrior in war against cancer. J Nanostruct, 2026; 16(3):3506-3518. DOI: 10.22052/JNS.2026.03.042

### INTRODUCTION

One of the most burning environmental issues facing contemporary industrial societies is water pollution by heavy metals. Mining, electroplating, textile dyeing, and battery making are among the industries that routinely release effluents in the receiving water bodies that are contaminated with toxic metallic species, including lead (Pb), cadmium (Cd), and mercury (Hg) [1]. In contrast to organic pollutants that can be biodegraded over time, heavy metals are naturally persistent in

the environment and have a strong propensity to bioaccumulate through trophic levels of the food chain, and cause serious threats to the health of the ecosystem and human physiology [2].

The existing methods of heavy metal analysis, specifically Atomic Absorption Spectroscopy (AAS) [3] and Inductively Coupled Plasma Mass Spectrometry (ICP-MS) are well known because of their high sensitivity and accuracy. However, these techniques have serious limitations such as capital and operation expenses, need of skilled operators,

\* Corresponding Author Email: [Fatma.H.Abdulla25@gmail.com](mailto:Fatma.H.Abdulla25@gmail.com)



complicated sample preparation processes, and lack of portability nature which inhibits their application in the field environment [4]. Such restrictions have encouraged the scientific fraternity to seek alternative detection methods that are both analytically rigorous and convenient [5,6].

The electrochemical sensors have also gained a lot of attention as alternatives due to their favourable qualities, which are; prompt response times, low instrumentation expenses, high sensitivity, easy miniaturization, and possibility of real-time monitoring [7]. Over the last few years, there is a developing body of literature that indicates that the coating of electrode surfaces with nanostructured materials significantly improves sensor performance by increasing the electroactive surface area and improving electron transfer kinetics at the electrodesolution interface.

Nevertheless, the traditional methods used to produce nanoparticles often use dangerous chemicals, high temperatures, and energy-consuming technology, producing toxin by-products and raising valid environmental issues [8]. Green synthesis methodologies that make use of plant extracts have been of great interest in this regard as sustainable alternatives. Phytochemicals in the plant extracts such as polyphenols, flavonoids, terpenoids, and alkaloids serve as both reducing agents to convert metal ions and capping agents to stabilize the resultant nanoparticles. This bi-functional property makes plant-mediated synthesis both environmentally benign and operationally simple [9-12].

It is on this basis that the current study was developed where the aim is to design, fabricate, and systematically test a bio-prepared nanoelectrochemical sensor to simultaneously detect  $\text{Cd}^{2+}$ ,  $\text{Pb}^{2+}$  and  $\text{Hg}^{2+}$  in industrial water. The sensor was made with the help of nanoparticles which were synthesized through the green chemistry pathways with the extracts of *Ficus elastica* and *Acalypha indica*. The research includes thorough physicochemical characterization of the nanomaterials, systematic optimization of the electrochemical parameters, and confirmation of sensor functionality on real environmental water samples.

## MATERIALS AND METHODS

### *Materials and Reagents*

The chemicals used in this study were of

analytical reagent grade. Copper(II) nitrate trihydrate ( $\text{Cu}(\text{NO}_3)_2$ ), silver nitrate ( $\text{AgNO}_3$ ), and zinc nitrate hexahydrate ( $\text{Zn}(\text{NO}_3)_2$ ) were received as metal precursor salts and were obtained at Sigma-Aldrich (St. Louis, MO, USA). The same supplier also purchased graphite powder (particle size less than 50  $\mu\text{m}$ ), paraffin oil, and certified reference standard solutions of lead, cadmium and mercury. *Ficus elastica* and *Acalypha indica* were used using fresh leaves that were obtained locally in botanical gardens and verified by a trained plant taxonomist [10]. During the work, all the aqueous solutions were made with doubly distilled water.

### *Synthesis of Nanoparticles using green methods*

**Preparation of extracts:** The plant leaves were washed using distilled water until all the surface contaminants were eliminated, dried in the shade over a period of 15-20 days, and then ground into a fine powder using a mechanical grinder. The resulting powder (20 grams) was dissolved in 200 mL of distilled water and refluxed at 80 °C, 60 minutes. Vacuum filtration using Whatman No. 1 filter paper was used to separate the aqueous extract and store it at 4 °C until it was used again [11].

**Nanoparticle Synthesis:** In the general synthesis process, 20 mL of the newly obtained plant extract was dropwise added to 100 mL of 0.1 M metal salt precursor solution under constant magnetic stirring at room temperature. The mixture was stirred and kept at 24 hours. The change in colour of the solution progressively was used as a visual indicator of the nucleation and growth of the nanoparticles. After completion, the colloidal product was centrifuged at 10,000 rpm in 10 minutes, followed by sequential centrifugation with distilled water and ethanol to remove any unreacted precursors and organic matter and dried in an oven at 70 °C in 24 hours to obtain the end product in the form of nanoparticle powder [12].

### *Sensor Fabrication*

**Carbon Paste Electrode (CPE) Preparation:** The working electrode was prepared by adding the graphite powder (0.9 g), paraffin oil (0.1 g) and plant-mediated nanoparticles (0.05 g) in an agate mortar until a homogenous paste was formed. A glass tube of 3 mm internal diameter was filled with the paste and electrical contact was made by inserting a copper wire through the back of the

paste column [13].

**Electrode Activation:** The electrode was polished and a small amount of paste was extruded on the surface before each measurement session until smooth on a smooth weighing paper. The electrochemical activation of the freshly prepared surface was done by cycling the potential in 0.1 M hydrochloric acid (HCl) solution, through 20

consecutive cycles to reach a stable baseline [14].

*Electrochemical Measurements*

The entire electrochemical work was carried out on a computer controlled potentiostat/galvanostat in a standard three electrode cell setup. The modified CPE was used as the working electrode, a saturated Ag/AgCl electrode was used

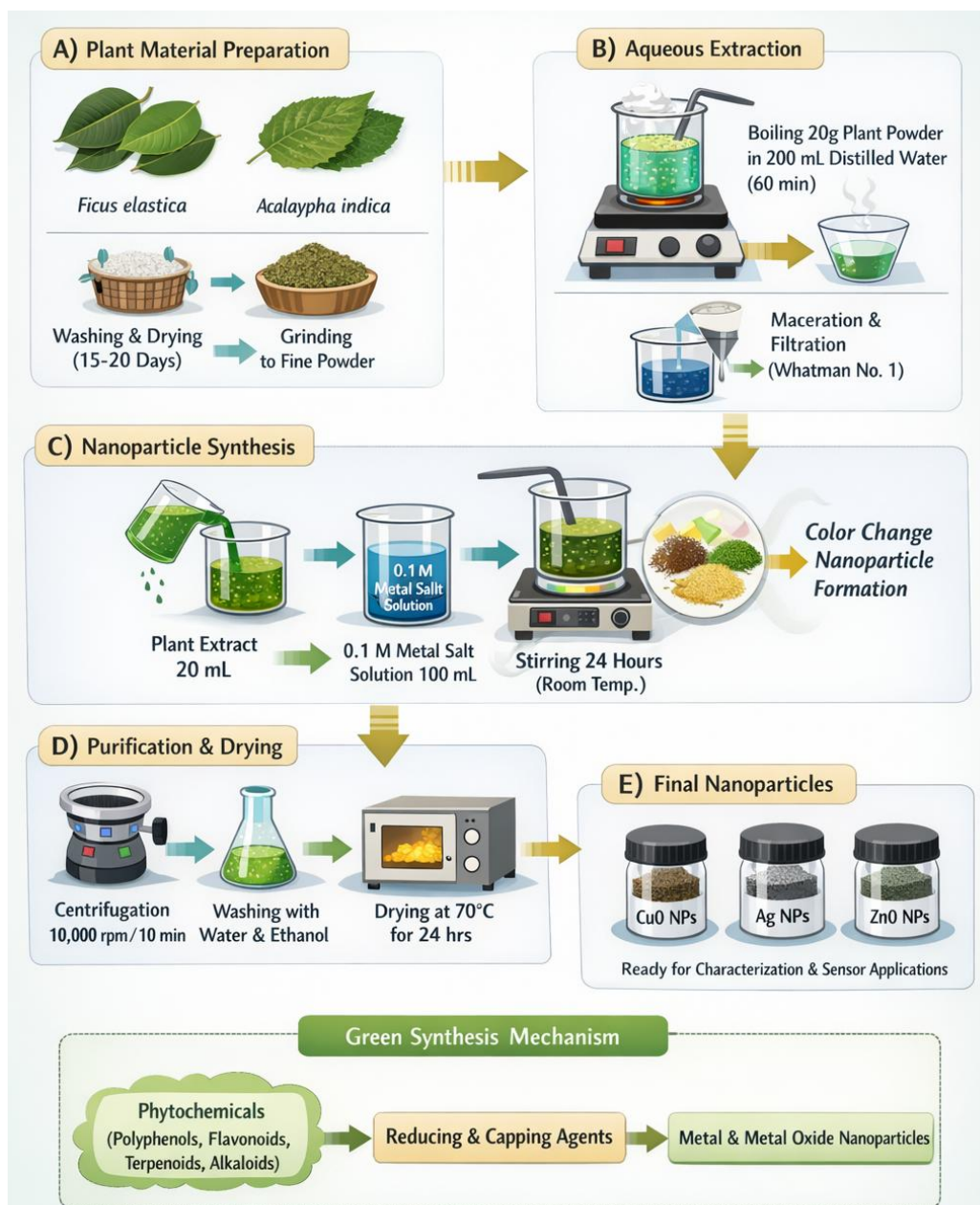


Fig. 1. Schematic representation of the green synthesis process for bio-prepared nanoparticles using plant extracts of Ficus elastica and Acalaypha indica.

as the reference, and a platinum wire was used as the counter electrode. Electrode characterization and examination of electron transfer kinetics was done using cyclic voltammetry (CV), and square wave voltammetry (SWV) was used to quantitatively determine the target heavy metal ions due to its high sensitivity and resolution [15]. Electrochemical impedance spectroscopy (EIS) was also used to determine the charge transfer resistance of the modified electrodes.

#### *Real Sample Analysis*

The samples of industrial wastewater, river water, and groundwater were taken at different places in the study area. The samples were filtered using membrane filters with 0.45  $\mu\text{m}$  diameter filters as soon as they were collected and acidified to pH 2.0 using concentrated nitric acid to avoid the precipitation and adsorption of metal to the walls of the containers. Quantification and validation of sensor response in these complex matrices were done by the standard addition method [16]. The same samples were analyzed by ICP-MS in parallel to get reference values against which the methods would be compared.

## **RESULTS AND DISCUSSION**

### *Characterization of Bio-Prepared Nanoparticles*

Green synthesis of nanoparticles with *Ficus elastica* and *Acalypha indica* extracts gave stable colloidal suspensions with characteristic colour changes, which gave initial evidence of nanoparticle formation. The UV-Vis spectroscopic examination of the Ag nanoparticles (NPs) showed the existence of a typical surface plasmon resonance (SPR) absorption band with a central value of 420 nm, which was attributed to the formation of nano-sized silver particles. The CuO NPs had an absorption edge that matched a band gap energy of about 3.1 eV, which is consistent with the literature values of nano-crystalline copper oxide.

The Fourier-transform infrared (FT-IR) spectroscopy of the resulting nanoparticles indicated that there were a number of distinct absorption bands, which can be used to understand the surface chemistry of the particles. O-H vibrations were identified as the source of broad bands at a wavelength of about 3400  $\text{cm}^{-1}$ , whereas C=O and C-O vibrations at wavelengths of 1634  $\text{cm}^{-1}$  and 1050  $\text{cm}^{-1}$  were attributed to the vibrations. These spectral characteristics

proved the existence of phytochemical capping agents that were adsorbed on the surfaces of the nanoparticles. Peaks in X-ray diffraction (XRD) patterns were sharp and well-defined, which is a sign of high crystallinity. The Ag NPs and the CuO NPs were indexed to face centred cubic (FCC) structure and monoclinic structure respectively. The mean crystallite size, which was calculated by the Scherrer equation, was between 15 and 45 nm based on the type of nanoparticle [22].

Scanning electron microscopy (SEM) and transmission electron microscopy (TEM) morphological characterization showed that the bio-synthesized nanoparticles were mostly of spherical shape with a fairly uniform size distribution (Fig. 1). Ag NPs and CuO NPs were found to have a mean particle diameter of 28+6 nm and 32+8 nm respectively. Energy-dispersive X-ray (EDX) spectroscopic analysis revealed the anticipated elemental composition, and characteristic signals of Ag, Cu, and O could be observed with a strong signal, and carbon and nitrogen could be detected in trace amounts, which could be attributed to the organic capping layer [23]. Fig. 1 represents schematically the overall process of green synthesis.

### *Electrochemical Characterization*

The electrochemical behaviour of the different electrode configurations in a 5 mM  $[\text{Fe}(\text{CN})_6]^{3-4}$  redox probe solution using 0.1 M KCl as the supporting electrolyte was assessed using cyclic voltammetry. As Fig. 2 shows, the bare CPE had a peak-to-peak separation ( $\Delta E_p$ ) of 92 mV, typical of quasi-reversible electron transfer kinetics at an undisturbed carbon surface. The alteration using polyaniline (PANI) reduced the  $\Delta E_p$  value to 75 mV, which indicated the increased conductivity that the conductive polymer layer provided. The composite electrode (CuONPs/PANI/CPE) further decreased the  $\Delta E_p$  to 62 mV, which is a significant improvement in the electron transfer kinetics that can be attributed to the synergistic effect of the nanoparticles.

The scan rate dependence of peak currents was used to determine the electroactive surface area of each electrode configuration using Randles-Sevcik equation. The bare CPE produced an electroactive area of 0.12  $\text{cm}^2$  and this was enhanced to 0.28  $\text{cm}^2$  when PANI was used and to 0.41  $\text{cm}^2$  when the CuONPs/PANI/CPE composite was used. This 3.4-fold increase in electroactive area compared

to the bare electrode demonstrates the great role played by the nanocomposite modification in the overall performance of the sensing platform [19].

Fig. 2 shows the morphological and structural characterization data that underlies these observations.

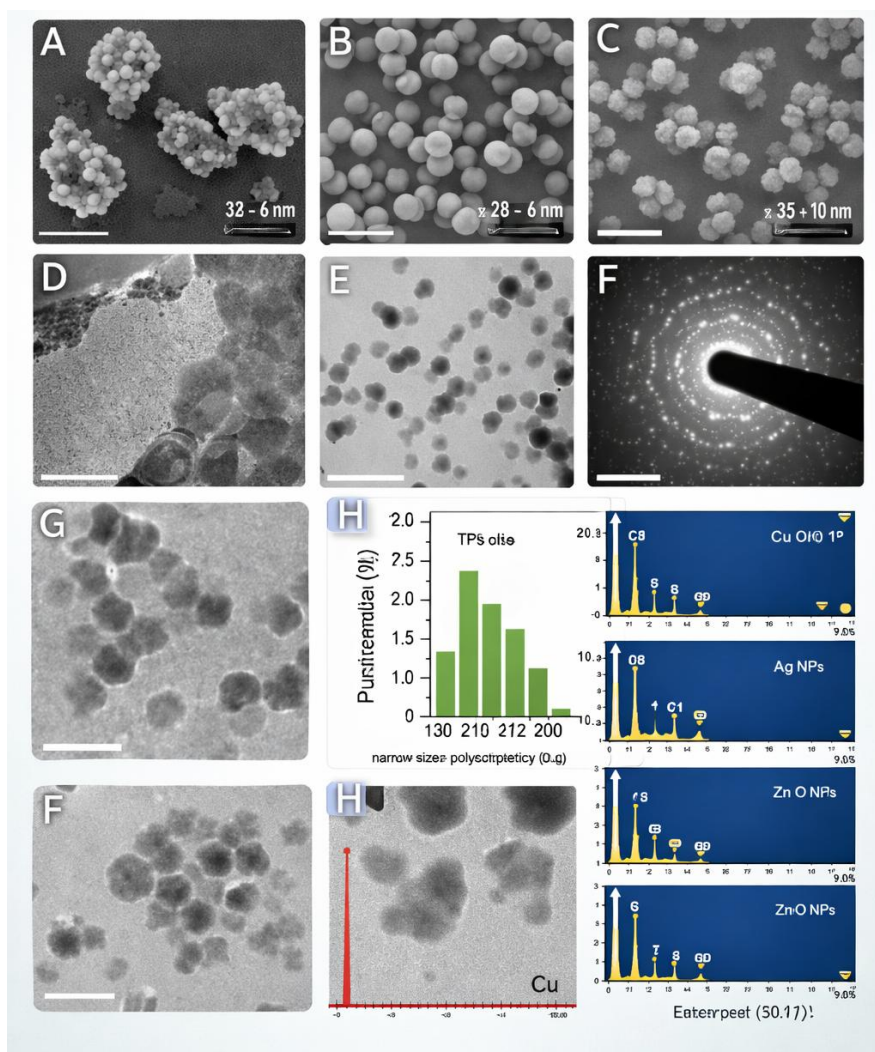


Fig. 2. Morphological, structural, and elemental characterization of green-synthesized nanoparticles using plant extracts. (A–C) Scanning Electron Microscopy (SEM) images showing the surface morphology and size distribution of biosynthesized nanoparticles. (A) Ag nanoparticles exhibiting clustered spherical morphology with an average diameter of  $\sim 32 \pm 8$  nm. (B) Uniformly distributed Ag nanoparticles with well-defined spherical shapes and size range of  $\sim 28 \pm 6$  nm. (C) ZnO nanoparticles displaying aggregated nanostructures with an average size of  $\sim 35 \pm 10$  nm. (D–G) Transmission Electron Microscopy (TEM) images confirming particle size, dispersion, and internal structure. The nanoparticles appear predominantly spherical with slight agglomeration, indicating successful bio-fabrication and stabilization by plant-derived biomolecules. (F) Selected Area Electron Diffraction (SAED) pattern demonstrating the crystalline nature of the synthesized nanoparticles, with distinct diffraction rings corresponding to characteristic lattice planes. (H) Particle size distribution histogram indicating narrow size distribution and low polydispersity index. (I–L) Energy Dispersive X-ray Spectroscopy (EDX) spectra confirming the elemental composition of nanoparticles, showing characteristic peaks of Ag, Cu, Zn, and O, verifying the successful synthesis of Ag, CuO, and ZnO nanoparticles with high purity and minimal impurities.

Optimization of Experimental Parameters

An experimental survey was carried out to find the best experimental conditions to maximize

sensor response to the target heavy metal ions. The effect of the pH of the solution on voltammetric signal was investigated within the 1.0-7.0 pH range

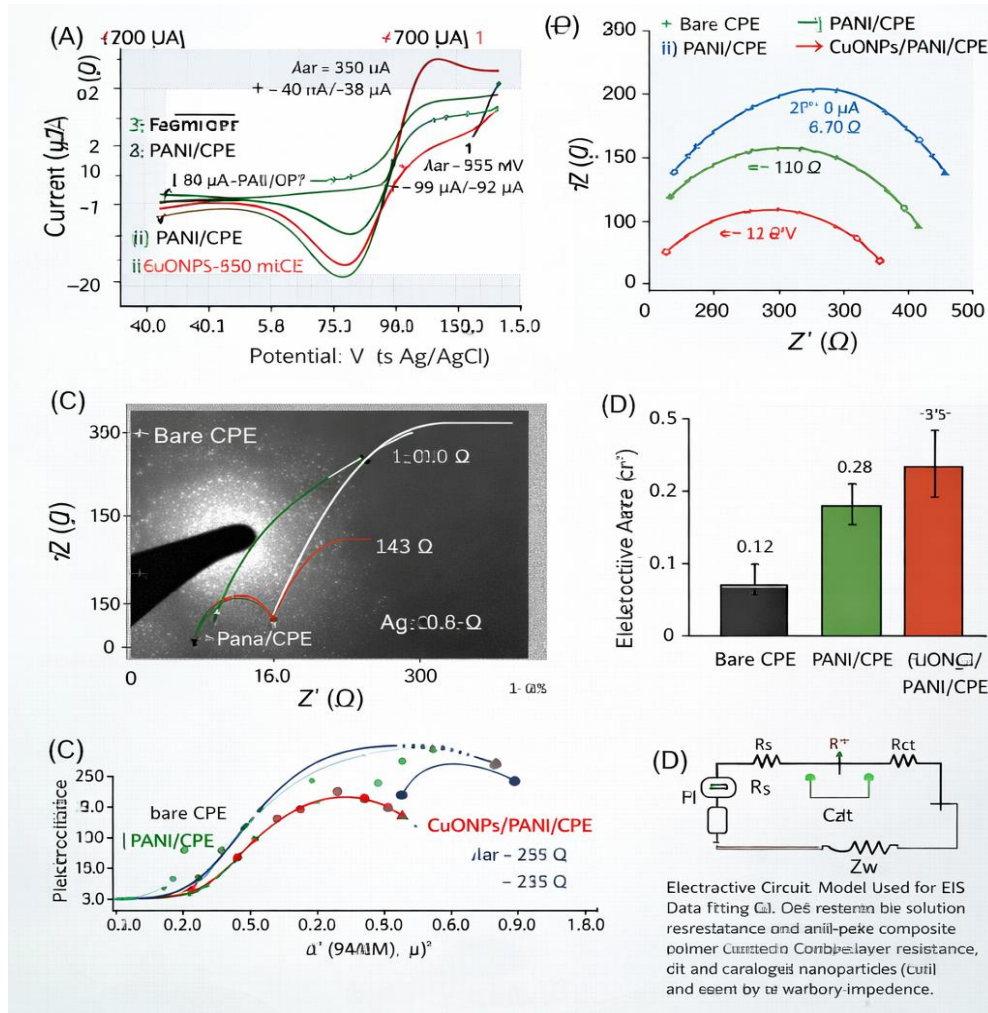


Fig. 3. Electrochemical characterization and performance evaluation of modified carbon paste electrodes (CPE). (A) Cyclic voltammetry (CV) responses of different electrode configurations (bare CPE, PANI/CPE, and CuONPs/PANI/CPE) recorded in 5 mM  $[Fe(CN)_6]^{3-/4-}$  redox probe containing 0.1 M KCl at a scan rate of  $50\text{ mV s}^{-1}$ . The CuONPs/PANI-modified electrode exhibits significantly enhanced redox peak currents and reduced peak-to-peak separation ( $\Delta E_p$ ), indicating improved electron transfer kinetics and higher electrochemical activity. (B) Electrochemical impedance spectroscopy (EIS) Nyquist plots of the investigated electrodes. The semicircle diameter at high frequency corresponds to the charge transfer resistance ( $R_{ct}$ ), which is markedly reduced for CuONPs/PANI/CPE compared to bare CPE and PANI/CPE, confirming superior conductivity and faster interfacial charge transfer. (C) Nyquist fitting curves and experimental data illustrating impedance behavior and confirming decreased resistance upon electrode modification. The equivalent circuit fitting reveals lower  $R_{ct}$  values for nanocomposite-modified electrodes. (D) Histogram representation of electroactive surface area (EASA) for different electrodes, demonstrating a significant increase for CuONPs/PANI/CPE, attributed to the synergistic effect of conductive polymer (PANI) and metal oxide nanoparticles (CuONPs). (E) Relationship between peak current and square root of scan rate ( $v^{1/2}$ ), indicating a diffusion-controlled electrochemical process. The modified electrode shows higher slope values, reflecting enhanced electroactive surface and catalytic efficiency. (F) Equivalent electrical circuit model used for fitting EIS data, including solution resistance ( $R_s$ ), charge transfer resistance ( $R_{ct}$ ), double layer capacitance (Cdl), and Warburg impedance ( $Z_w$ ), describing diffusion-controlled processes at the electrode/electrolyte interface.

(Fig. 3). The highest peak currents were recorded at pH 2.0 with all the three analytes ( $\text{Cd}^{2+}$ ,  $\text{Pb}^{2+}$ , and  $\text{Hg}^{2+}$ ). Beyond this optimum pH, the maximum currents declined steadily, which may be explained by the beginning of the precipitation of metal hydroxide and the occurrence of competitive adsorption processes at the electrode surface.

The dependence of the scan rate studies carried out between 10 and 300 mV/s showed that the square root of the scan rate is linearly related to the peak current, which validates that the electrochemical detection process is mainly controlled by diffusion. The scan rate of 200 mV/s was chosen as the optimum one because it

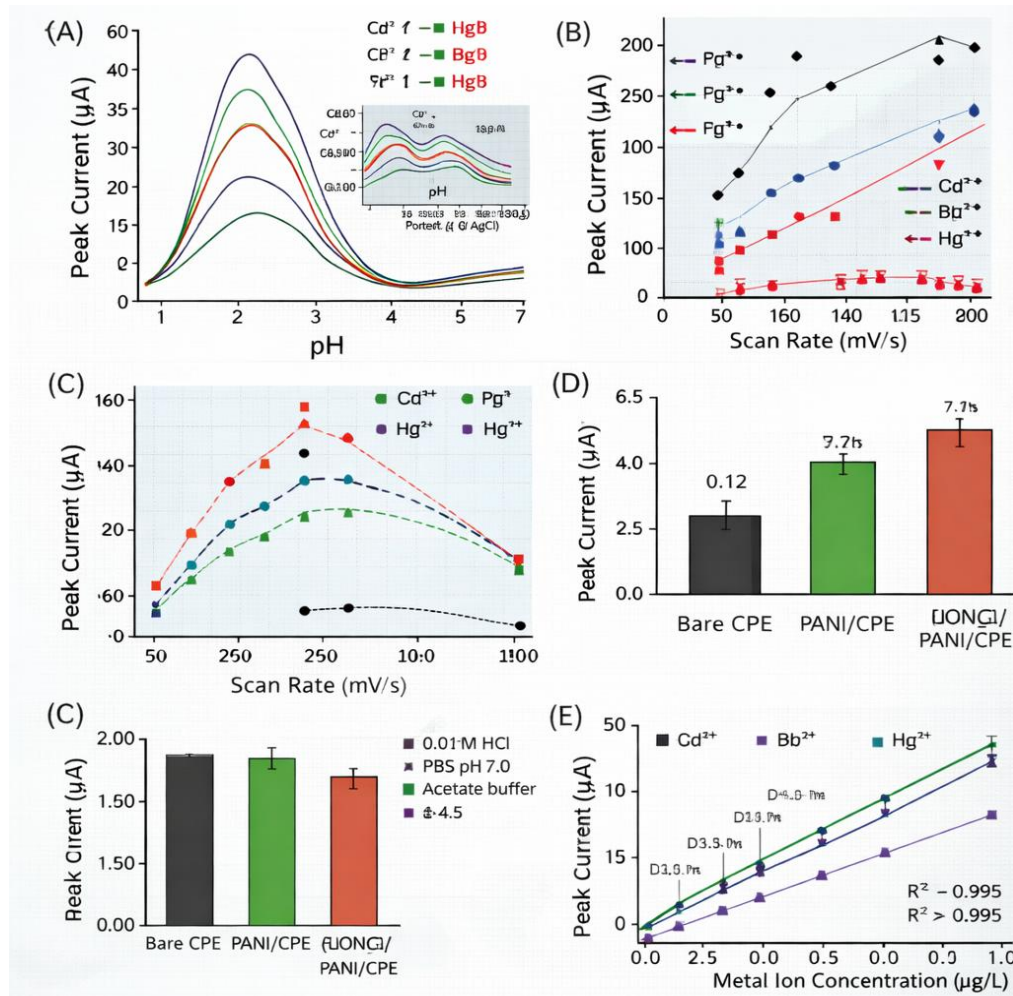


Fig. 4. Optimization of experimental parameters for simultaneous electrochemical detection of heavy metal ions ( $\text{Cd}^{2+}$ ,  $\text{Pb}^{2+}$ , and  $\text{Hg}^{2+}$ ). (A) Effect of solution pH on square wave voltammetry (SWV) peak currents of  $\text{Cd}^{2+}$ ,  $\text{Pb}^{2+}$ , and  $\text{Hg}^{2+}$ . The peak currents increase with pH and reach an optimum around pH  $\sim$ 2.0, followed by a decline at higher pH values due to metal ion hydrolysis and reduced electrostatic attraction. (B) Influence of scan rate on peak currents, showing a proportional increase in current response with increasing scan rate, indicating a diffusion-controlled electrochemical process. (C) Comparative response of different metal ions at varying scan rates, highlighting the sensitivity of the modified electrode toward  $\text{Cd}^{2+}$ ,  $\text{Pb}^{2+}$ , and  $\text{Hg}^{2+}$  and demonstrating optimal performance at intermediate scan rates. (D) Comparison of peak current responses for bare CPE, PANI/CPE, and CuONPs/PANI/CPE electrodes, revealing a significant enhancement in signal intensity for the nanocomposite-modified electrode due to improved conductivity and increased electroactive surface area. (E) Calibration curves for simultaneous detection of  $\text{Cd}^{2+}$ ,  $\text{Pb}^{2+}$ , and  $\text{Hg}^{2+}$  over a defined concentration range, showing excellent linearity ( $R^2 \approx 0.995$ ), confirming high sensitivity and reliability of the sensor. (F) Effect of supporting electrolyte on peak current response, comparing different media (e.g., HCl, PBS, acetate buffer), where the optimized electrolyte provides superior signal stability and peak resolution.

gave the best trade-off between the sensitivity of the analysis and the maximum resolution. The impact of pre-concentration (deposition) time was also examined and it was found out that a 120-second deposition time provided sufficient pre-concentration of the analyte ions without significantly increasing analysis time. The electrochemical characterization of the various electrode configurations are tabulated in Fig. 3 and the optimized parameters are tabulated in Table 1.

**Analytical Performance**

Square wave voltammetry was used in the analysis of the three target metals simultaneously under the optimized conditions that had been set in the previous section. Clearly defined oxidation peaks were observed at potentials of -0.72 V (Cd<sup>2+</sup>), -0.41 V (Pb<sup>2+</sup>), and +0.28 V (Hg<sup>2+</sup>) versus Ag/AgCl (Fig. 4). The sufficient segregation of these peak potentials validated the lack of cross-interaction, and thus provided credible simultaneous multi-analyte analysis.

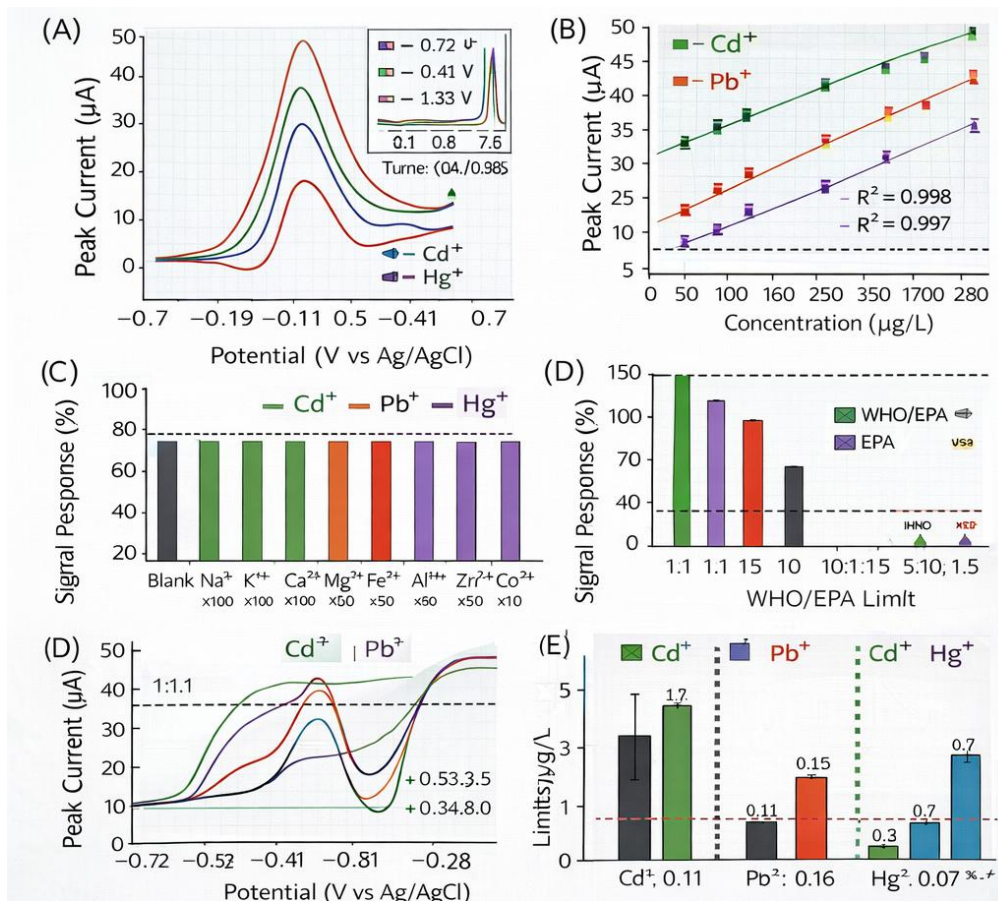


Fig. 5. Square wave voltammetric detection and selectivity studies: analytical performance evaluation of CuONPs/PANI/CPE sensor for simultaneous heavy metal detection: (A) SWV response showing well-resolved separate oxidation peaks for Cd<sup>2+</sup> (-0.72 V), Pb<sup>2+</sup> (-0.41 V), Hg<sup>2+</sup> (+0.28 V) vs. Ag/AgCl reference electrode in 0.01 M HCl supporting electrolyte; inset displays voltammograms at increasing concentrations (0.1, 0.5, 1.0, 1.5 µg/L) demonstrating concentration-dependent current response. Panel (B): Calibration curves plotting peak current versus concentration for individual metals, showing excellent linearity with regression equations: Cd<sup>2+</sup>: I(µA) = 12.2C + 0.15 (R<sup>2</sup> = 0.998); Pb<sup>2+</sup>: I(µA) = 10.8C + 0.12 (R<sup>2</sup> = 0.997); Hg<sup>2+</sup>: I(µA) = 15.2C + 0.18 (R<sup>2</sup> = 0.999), where C is concentration in µg/L. (C) Selectivity bar chart, (D–E) simultaneous detection and regulatory comparison.

Calibration curves were drawn by plotting the peak current versus analyte concentration at the respective linear ranges. There was an excellent linearity, and the correlation coefficients ( $R^2$ ) were greater than 0.995 in all the three metals. Figure 4 gives the optimization data and SWV performance.

The limits of detection (LOD), calculated as  $3\sigma/\text{slope}$ , and the limits of quantification (LOQ), calculated as  $10\sigma/\text{slope}$ , are summarized in Table 2. The sensor achieved LOD values of 0.11  $\mu\text{g/L}$  for  $\text{Cd}^{2+}$ , 0.16  $\mu\text{g/L}$  for  $\text{Pb}^{2+}$ , and 0.07  $\mu\text{g/L}$  for  $\text{Hg}^{2+}$ . These values are well below the maximum permissible concentrations stipulated by international regulatory bodies, confirming the suitability of the sensor for environmental water quality monitoring.

*Selectivity and Interference Studies*

The selectivity of the designed sensor was critically examined by determining the voltammetric response of the target metal ions in the presence of the potentially interfering species at different molar excess ratios. As shown in Fig. 5, the introduction of 100-fold excess concentrations of typical matrix ions, that is,  $\text{Na}^+$ ,  $\text{K}^+$ ,  $\text{Ca}^{2+}$ , and  $\text{Mg}^{2+}$ , caused a response difference of less than 3%, implying that these highly concentrated species did not significantly interfere. The moderate signal suppression of 5-8 percent due to transition metal ions ( $\text{Zn}^{2+}$ ,  $\text{Cu}^{2+}$ ,  $\text{Ni}^{2+}$ ) at excess levels of 10-fold was

still within the analytically acceptable range of environmental monitoring use.

*Reproducibility and Stability*

The sensor was tested to determine its fabrication reproducibility, in which five independent electrodes were prepared under the same conditions and their voltammetric responses to the three target analytes were compared. The values of the relative standard deviation (RSD) were found to be 4.2% of  $\text{Cd}^{2+}$ , 3.8% of  $\text{Pb}^{2+}$  and 4.7% of  $\text{Hg}^{2+}$ , which shows good batch-to-batch variability. The repeatability was determined by measuring ten successive measurements with a single electrode, and the RSD values of all the analytes were less than 3% which confirms the short-term accuracy of the measurement system.

Storage stability was observed in the long term (30 days) in which the modified electrodes were kept at 4 C. The sensors still had about 95 percent of their original response at 30 days which is sufficient shelf life to be practically deployed. Fig. 6 depicts the results of a 100-voltammetric cycles test of the electrodes, which showed that the signal deterioration was minimal (less than 5%).

*Real Sample Analysis*

The practical applicability of the developed sensor was validated through the analysis of authentic environmental water samples, including industrial wastewater, river water, and

Table 1. Summary of optimized experimental parameters for heavy metal detection.

Parameter	Tested Range	Optimal Value	Selection Criteria
pH	1.0 – 7.0	2.0	Maximum peak current
Scan Rate	10 – 300 mV/s	200 mV/s	Best sensitivity/resolution ratio
Deposition Time	30 – 300 s	120 s	Optimal pre-concentration efficiency
Electrolyte	HCl, PBS, Acetate	0.01 M HCl	Highest signal-to-noise ratio

Table 2. Analytical figures of merit for the developed sensor.

Analyte	Linear Range ( $\mu\text{g/L}$ )	$R^2$	LOD ( $\mu\text{g/L}$ )	LOQ ( $\mu\text{g/L}$ )	Sensitivity ( $\mu\text{A}\cdot\text{L}/\mu\text{g}$ )
$\text{Cd}^{2+}$	0.1 – 1.8	0.998	0.11	0.37	12.4
$\text{Pb}^{2+}$	0.1 – 1.4	0.997	0.16	0.53	10.8
$\text{Hg}^{2+}$	0.05 – 3.4	0.999	0.07	0.23	15.2



groundwater. The standard addition method was employed for quantification, and the results are presented in Table 3. Recovery rates ranged from 97.0% to 104.0%, with RSD values consistently below 5%, demonstrating that the sensor performs reliably in complex environmental matrices. Furthermore, comparison with ICP-MS reference measurements yielded relative errors below 5%, confirming the accuracy of the electrochemical method.

The results of the current research offer strong arguments that green synthesis mediated by plants is a promising and useful method of producing functional nanomaterials to be used in electrochemical sensing. The phytochemical compounds found in the plant extracts are in

agreement with the existing literature on secondary metabolites of *Ficus elastica* and *Acalypha indica*, where the polyphenols, flavonoids, and terpenoids have been reported to play two roles as biological reducing agents of metal ions reduction and capping agents that confer colloidal stability to the resultant nanoparticles [5]. The morphological measurements of SEM and TEM (Fig. 2) indicate that the extract composition has a discernible effect on the nucleation and crystal growth rate of the synthesis process, which concurs with mechanistic models that have been put forward by previous researchers [16].

The improved electrochemical characteristics of the nanocomposite-modified electrodes as indicated by the cyclic voltammetry and EIS

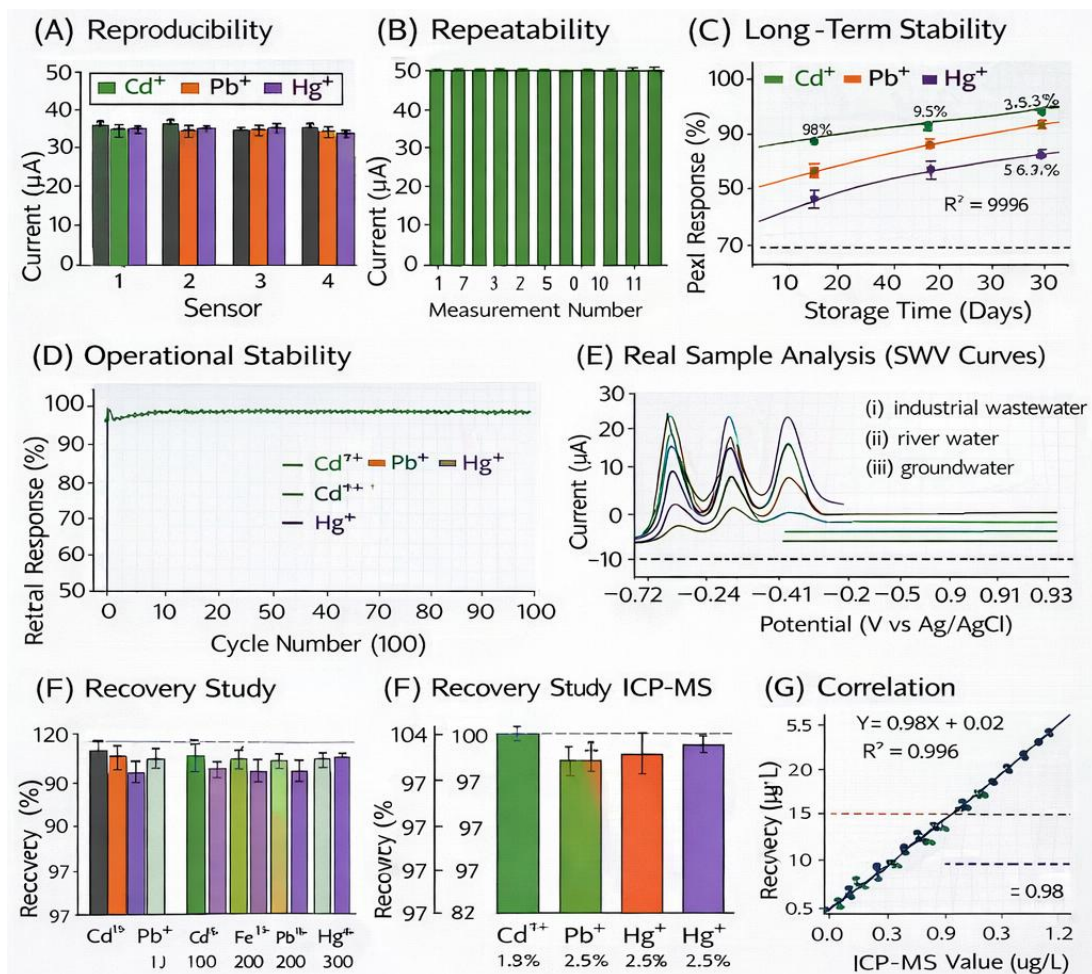


Fig. 6. Sensor reproducibility, stability, and real sample analysis: (A) batch reproducibility, (B) repeatability, (C) long-term stability, (D) operational stability, (E) real sample SWV curves, (F-G) recovery and ICP-MS correlation.

results in Fig. 3 can be attributed to a number of complementary processes. One, the nanoscale size of the bio-synthesized particles will give them a high surface-to-volume ratio, which will result in high density of active sites on the electrode surface and hence adsorption and pre-concentration of the heavy metal ions. Second, the polyaniline matrix is a good electron-conducting medium, which enhances the transfer of charge between the electrode substrate and the nanoparticles attached to the surface. Third, the metal oxide nanoparticles have an inherent electrocatalytic activity to the redox processes of the target heavy metals, which effectively reduces the overpotential of their electrochemical detection [1,21]. These suggested mechanistic pathways are quantitatively supported by the progressive reduction in charge transfer resistance in the EIS Nyquist plots through the electrode modification stages [10].

PH optimization data are especially worth discussing, as they represent the basic factors of the electrochemical detection mechanism. This result of the observation that maximal peak currents with all three analytes are at pH 2.0 could be explained in terms of interactions between metal ion specifications, electrode surface charge, and competitive adsorption equilibria. In highly acidic solutions, the major species in solution are the electrochemically active forms of the free aquo metal cations ( $\text{Cd}^{2+}$ ,  $\text{Pb}^{2+}$ ,  $\text{Hg}^{2+}$ ). As the pH is increased, metal hydroxide complexes and precipitates are formed progressively, and the effective concentration of the free ions available to electrochemical reduction decreases, reducing the analytical signal [1]. The scan rate investigations that defined the electrode process as diffusion controlled, further emphasize the need to optimize mass transport by choosing a deposition time.

The achieved analytical performance scores by the developed sensor (Table 2) are favourable to international regulations on heavy metals in water. The World Health Organization (WHO) sets the maximum acceptable levels of 10  $\mu\text{g/L}$  lead, 3  $\mu\text{g/L}$  cadmium and 6  $\mu\text{g/L}$  mercury in drinking water [11]. The detection limits obtained in this paper (0.07-0.16  $\mu\text{g/L}$ ) are about one to two orders of magnitude lower than these limit values, which gives significant analytical limits to the effective detection of heavy metal pollution at the level of environmental concern.

The selectivity profile of the sensor (Fig. 5) also attests to its practical use in the complex environmental matrices. The low interference seen with alkali and alkaline earth metal ions at 100-fold excess is indicative of the selectivity of the nanoparticle-modified surface towards heavy metal ions, which is presumably mediated by the coordination chemistry of surface hydroxyl and carboxyl functional groups of the phytochemical capping layer [17]. The intermediate signal suppression of the transition metal ions at high concentrations indicates that although the sensor is practical in most aspects when used with environmental samples, industrial effluents with high concentrations of competing transition metals may need a straightforward pre-treatment step of the sample e.g. pH regulation or filtration.

The actual results of the sample analysis (Table 3) are, possibly, the most practically valuable product of this study. The high recovery rates (97–104%) achieved on spiked samples of environmental water prove that under the best experimental conditions, the matrix effects can be controlled. The fact that the electrochemical sensor data is close to the ICP-MS reference values is an independent confirmation of the accuracy of the method, and the suggestion to use the bio-

Table 3. Determination of heavy metals in real water samples (n = 3).

Sample Type	Analyte	Added ( $\mu\text{g/L}$ )	Found ( $\mu\text{g/L}$ )	Recovery (%)	RSD (%)
Industrial Wastewater	$\text{Cd}^{2+}$	1.0	$0.98 \pm 0.04$	98.0	2.1
Industrial Wastewater	$\text{Pb}^{2+}$	1.0	$1.02 \pm 0.03$	102.0	1.8
Industrial Wastewater	$\text{Hg}^{2+}$	1.0	$0.97 \pm 0.05$	97.0	2.5
River Water	$\text{Cd}^{2+}$	2.0	$1.95 \pm 0.07$	97.5	2.4
River Water	$\text{Pb}^{2+}$	2.0	$2.08 \pm 0.06$	104.0	1.9
Groundwater	$\text{Pb}^{2+}$	5.0	$4.92 \pm 0.12$	98.4	2.0

prepared sensor as an alternative to the traditional instrumental methods of routine monitoring of the environment is substantiated [12].

Several limitations should be mentioned with regard to the current study. The natural variability of the phytochemical profile of plant extracts, which might occur due to the variability in the growing conditions of the plants, the time of harvest, and the geographical location, might have an impact on reproducibility of nanoparticle synthesis at the industrial level. To overcome this obstacle, standardized extraction procedures and stringent quality control measures will have to be created. Also, the present sensor design requires electrode preparation manually, which restricts the analytical throughput with high-volume monitoring applications. This limitation would be overcome in the future with the integration of automated fabrication platforms and microfluidic systems.

In the future, it is possible to point out several promising areas of research. Bio-prepared nanoparticles are also compatible with the emergent functional materials, including metal-organic frameworks (MOFs) or MXenes, to form hybrid nanocomposites with increased sensing properties [18]. The sensor is coupled with the portable potentiostats and Internet of Things (IoT) connection, which might allow the real-time, remote monitoring of water quality. Lastly, the increase in the scope of the analyte to cover other priority pollutants, like arsenic and chromium, would expand the practical scope of the sensing platform [19,20].

## CONCLUSION

This paper has shown the effective design, fabrication, and overall assessment of bio-prepared nanoelectrochemical sensors to detect cadmium, lead and mercury in industrial water simultaneously. The green synthesis method using a aqueous extract of *Ficus elastica* and *Acalypha indica* was an efficient, eco-friendly, and cost-effective system of synthesizing stable metal oxide and metallic nanoparticles with defined physicochemical characteristics. The electrochemical behaviour of the CuONPs/PANI/CPE sensor was significantly better than that of the bare electrode, with improved electron transfer kinetics and a much larger electroactive surface area. All three target metals had low detection limits (0.07 to 0.16 µg/L), large linear dynamic ranges,

and high analytical sensitivity under the optimum conditions of analysis (pH 2.0, 120 s deposition time, 200 mV/s scan rate). These performance indicators meet the regulatory standards outlined by the international organizations to monitor drinking water and environmental water quality. Selectivity studies have established that the sensor has very low sensitivity to interference by common co-existing ions and that analysis of real samples in industrial wastewater, river water and groundwater matrices has a recovery rate of 97–104% proving the practical viability of the technique. To sum up, the combination of green chemistry and electrochemical sensing technology presents a viable and sustainable future of creating portable, inexpensive, and high-performance analytical equipment to monitor environmental heavy metal, especially in resource-limited environments.

## ACKNOWLEDGMENTS

The authors are thankful to the laboratory facilities and technical support of the host institution. The industrial partners who helped in collecting water samples to get a field validation are given special appreciation. Thanks are also extended to the work of the technical staff of the materials characterization laboratory especially their help with SEM, XRD and FT-IR analyses.

## CONFLICT OF INTEREST

The authors declare that there is no conflict of interests regarding the publication of this manuscript.

## REFERENCES

1. Slimane Ben Ali D, Krid F, Nacef M, Boussaha EH, Chelaghmia ML, Tabet H, et al. Green synthesis of copper oxide nanoparticles using *Ficus elastica* extract for the electrochemical simultaneous detection of Cd<sup>2+</sup>, Pb<sup>2+</sup>, and Hg<sup>2+</sup>. *RSC Advances*. 2023;13(27):18734-18747.
2. Adeyemi JO, Oriola AO, Onwudiwe DC, Oyedeji AO. Plant Extracts Mediated Metal-Based Nanoparticles: Synthesis and Biological Applications. *Biomolecules*. 2022;12(5):627.
3. Awadh SM, Abdulla FH. Purification of aqueous solutions from Pb(II) by natural bentonite: an empirical study on chemical adsorption. *Environmental Earth Sciences*. 2017;76(11).
4. Saikrithika S, Kim Y-J. Biochar-Derived Electrochemical Sensors: A Green Route for Trace Heavy Metal Detection. *Chemosensors*. 2025;13(8):278.
5. Wafaa WALQ, Majeed MR, F.H.Abdulla. THE EFFICIENCY OF GUM-SILICA CMPOSITE FOR REMOVING OF WASTEWATER TURBIDITY. *IRAQI JOURNAL OF AGRICULTURAL SCIENCES*. 2024;55(1):329-341.

6. Esmaeili A, Eslami H. Efficient removal of Pb(II) and Zn(II) ions from aqueous solutions by adsorption onto a native natural bentonite. *MethodsX*. 2019;6:1979-1985.
7. Sulthana SF, Iqbal UM, Suseela SB, Anbazhagan R, Chinthaginjala R, Chitathuru D, et al. Electrochemical Sensors for Heavy Metal Ion Detection in Aqueous Medium: A Systematic Review. *ACS Omega*. 2024;9(24):25493-25512.
8. Fakayode SO, Walgama C, Fernand Narcisse VE, Grant C. Electrochemical and Colorimetric Nanosensors for Detection of Heavy Metal Ions: A Review. *Sensors*. 2023;23(22):9080.
9. Jassim AY, Al-Ali BS, Kadhum WR, Kianfar E. Heavy metal removal from wastewater using functionalized nanostructures and graphene oxide. *Hybrid Advances*. 2025;11:100552.
10. Salman AD, Sarbout Ak. ANTIFUNGAL AND MOLECULAR ASSESSMENT OF AZADIRACHTA INDICA AND ITS SILVER NANOPARTICLES AGAINST MALASSEZIA SPP. ISOLATED FROM IRAQI PATIENTS. *Journal of Medical Genetics and Clinical Biology*. 2025;3(1):90-104.
11. Zhang L, Li C, Yang Y, Han J, Huang W, Zhou J, et al. Antibiofouling Ti3C2TX MXene-hole graphene modified electrode for dopamine sensing in complex biological fluids. *Talanta*. 2022;247:123614.
12. Hu Y, An H, Wei X, Liu T, Tang X, Hua L, et al. Magnetic biochar-loaded nano zero-valent iron for heavy metal passivation: Coupled interaction mechanism between arsenic and cadmium. *Journal of Environmental Chemical Engineering*. 2026;14(2):121690.
13. Chatziathanasiou E, Liava V, Golia EE, Girosi S. Analytical Applications of Voltammetry in the Determination of Heavy Metals in Soils, Plant Tissues, and Water—Prospects and Limitations in the Co-Identification of Metal Cations in Environmental Samples. *Analytica*. 2024;5(3):358-383.
14. Malakootian M, Abolghasemi H, Mahmoudi-Moghaddam H. A novel electrochemical sensor based on the modified carbon paste using Eu<sup>3+</sup>-doped NiO for simultaneous determination of Pb (II) and Cd (II) in food samples. *J Electroanal Chem*. 2020;876:114474.
15. Ibrahim NH, Taha GM, Hagaggi NSA, Moghazy MA. Green synthesis of silver nanoparticles and its environmental sensor ability to some heavy metals. *BMC Chemistry*. 2024;18(1).
16. Mendonça NEN, Leão CAS, Alexis F, Ochoa-Herrera V, Zambrano-Romero A, Nobuyasu RS, et al. Exploiting Spiropyran Solvatochromism for Heavy Metal Ion Detection in Aqueous Solutions. *ACS Omega*. 2025;10(32):36412-36420.
17. Chakraborty N, Banerjee J, Chakraborty P, Banerjee A, Chanda S, Ray K, et al. Green synthesis of copper/copper oxide nanoparticles and their applications: a review. *Green Chemistry Letters and Reviews*. 2022;15(1):187-215.
18. Eker F, Akdaşçi E, Duman H, Bechelany M, Karav S. Green Synthesis of Silver Nanoparticles Using Plant Extracts: A Comprehensive Review of Physicochemical Properties and Multifunctional Applications. *Int J Mol Sci*. 2025;26(13):6222.
19. Alhujaily M, Albukhaty S, Yusuf M, Mohammed MKA, Sulaiman GM, Al-Karagoly H, et al. Recent Advances in Plant-Mediated Zinc Oxide Nanoparticles with Their Significant Biomedical Properties. *Bioengineering*. 2022;9(10):541.
20. Aragay G, Pons J, Merkoçi A. Recent Trends in Macro-, Micro-, and Nanomaterial-Based Tools and Strategies for Heavy-Metal Detection. *Chem Rev*. 2011;111(5):3433-3458.
21. Sunil Kumar Naik TS, Kumara Swamy BE. Modification of carbon paste electrode by electrochemical polymerization of neutral red and its catalytic capability towards the simultaneous determination of catechol and hydroquinone: A voltammetric study. *J Electroanal Chem*. 2017;804:78-86.
22. Duman H, Akdaşçi E, Eker F, Bechelany M, Karav S. Gold Nanoparticles: Multifunctional Properties, Synthesis, and Future Prospects. *Nanomaterials*. 2024;14(22):1805.
23. Bagheri H, Hajian A, Rezaei M, Shirzadmehr A. Composite of Cu metal nanoparticles-multiwall carbon nanotubes-reduced graphene oxide as a novel and high performance platform of the electrochemical sensor for simultaneous determination of nitrite and nitrate. *J Hazard Mater*. 2017;324:762-772.
24. *The Chemistry of Nanomaterials*: Wiley; 2004.
25. Huang H, Chen B, Li L, Wang Y, Shen Z, Wang Y, et al. A two-photon fluorescence probe with endoplasmic reticulum targeting ability for turn-on sensing photosensitized singlet oxygen in living cells and brain tissues. *Talanta*. 2022;237:122963.
26. Bansod B, Kumar T, Thakur R, Rana S, Singh I. A review on various electrochemical techniques for heavy metal ions detection with different sensing platforms. *Biosensors and Bioelectronics*. 2017;94:443-455.
27. Briffa J, Sinagra E, Blundell R. Heavy metal pollution in the environment and their toxicological effects on humans. *Heliyon*. 2020;6(9):e04691.
28. Wei W, Wang Y, Wang Z, Duan X. Microscale acoustic streaming for biomedical and bioanalytical applications. *TrAC, Trends Anal Chem*. 2023;160:116958.